LUIZ DONIZETE CAMPEIRO JUNIOR

TÍTULO: Avaliação e comparação da consolidação óssea com a utilização de biovidro F18 e enxerto autólogo em falha óssea induzida em rádio de galinhas domésticas

Relatório de Pós-doutorado realizado na Universidade Estadual Paulista "Júlio de Mesquita Filho" (UNESP), Faculdade de Medicina Veterinária e Zootecnia, Campus Botucat0

Supervisor(a): Profa. Titular Sheila Canevese Rahal

PROGRAMA DE PÓS-DOUTORADO DA UNESP

Botucatu

2026

Avaliação e comparação da consolidação óssea com a utilização de biovidro F18 e enxerto autólogo em falha óssea induzida em rádio de galinhas domésticas

"Evaluation and comparison of bone healing using F18 bioglass and autologous graft in induced bone failure in the radius of domestic chickens"

Abstract

This study aimed to evaluate, through radiographic and histological analyses, the performance of F18 bioglass putty in comparison with an autologous cortical bone graft for repairing radial bone defects in chickens, used here as an avian experimental model. A 0.5 cm midshaft defect was created in both radii of 30 adult chickens. In the left radius (G1), the defect was filled with F18 bioglass putty, whereas in the right radius (G2), the defect was filled with the bone fragment harvested from the left radius. Radiographs of the antebrachia were taken immediately after surgery and at 15, 30, 50, 60, and 90 days. Bone grafts appeared as well-defined radiopaque structures in all defects throughout the study. In contrast, F18 bioglass putty progressively diminished, from 100% detection at baseline to 6.7% at 90 days. The chickens were euthanized at 50, 90, and 120 days post-surgery to procedure histological examination. The statistical analysis revealed distinct treatment effects across different histological parameters. G1 showed significantly higher fibrocollagen proliferation intensity than G2, with odds about 6.4 times greater (86% vs. 51%, $p = 0.0037$), while no significant effects of time or treatment–time interaction were detected. Inflammatory infiltrate intensity was influenced by both treatment and time. G1 showed approximately 11 times higher odds of intense responses than G2. The highest intensities occurred at 50 days, with responses significantly greater than those at 90 and 120 days, and declined thereafter irrespective of treatment. Bone matrix formation displayed an opposite pattern, with G2 being about 22 times more likely to present high-intensity scores than G1, and no significant effects of time or interaction. For foreign body reaction, no differences were observed between groups, and neither treatment nor time influenced the response. In conclusion, autologous cortical bone graft and F18 bioglass putty exhibited distinct repair patterns, with the graft favoring bone matrix formation and the bioglass associated with greater fibrocollagen proliferation and inflammatory responses.

Keywords: bone repair, biomaterial, bioactive glass, histology.

1. Introduction

Bioactive materials are considered optimal for the development of bone tissue engineering scaffolds and for the repair or replacement of osseous structures; among them, bioactive glasses are particularly valued because they can be osteoconductive and, in certain formulations, osteoinductive (El-Rashidy et al., 2017). A systematic study showed that biomaterials based on bioactive glasses enhanced quantitative indicators of bone formation in critical-sized defects compared with untreated controls (Nozari et al., 2025). Different formulations of bioactive glass-based materials have been investigated, however, challenges persist in creating optimal compositions and ensuring their long-term stability in clinical settings (Ellakwa et al., 2025; Nozari et al., 2025).

A bioactive glass within the SiO_2–Na_2O–K_2O–CaO–MgO–P_2O_5 system with minor additives showed high stability against crystallization coupled with high bioactivity, which enabled the fabrication of flexible, bioresorbable fibers, meshes, and 3D structures for potential applications in soft and hard tissue regeneration (Souza et al., 2013; Souza et al., 2017). The morphological characteristics of this biomaterial, in the form of fibrous glassy scaffolds, were assessed in a rat tibial defect model, revealing increased expression of osteogenic factors and improved tibial callus strength 15 days post-surgery, suggesting its potential for bone repair (Gabbai-Armelin et al., 2015). Another study evaluated the mineralization potential of the fibrous glassy scaffold, demonstrating rapid formation of crystallized hydroxy-carbonate apatite, while in vitro biocompatibility assays showed enhanced proliferation of fibroblasts and osteoblasts without evidence of DNA damage, and subcutaneous implantation confirmed favorable soft tissue responses (Gabbai-Armelin et al., 2017).

F18 bioglass as putty was applied to segmental bone defects in the rabbit radius to evaluate its inductive capacity in the induced membrane technique, eliciting a foreign

body-type inflammatory response and membrane formation without the expansion potential required for the second stage of the Masquelet procedure (Silva Júnior et al., 2024). Subsequently, F18 bioactive glass-infiltrated Biosilicate® scaffolds (F18-17BioS) were developed, featuring an interconnected porous structure with porosity above 80%, a cell size of approximately 500 μm, and a compressive strength of 3.3 MPa—characteristics favorable for cell penetration, tissue ingrowth, vascularization, and effective nutrient delivery during bone healing (Marin et al., 2018).

Bone grafting aids fracture healing by supporting new bone formation (osteogenesis), stimulating bone-producing cells (osteoinduction), and providing a scaffold for bone growth (osteoconduction) (Bennett and Kuzma, 1992; Martin and Ritchie, 1994). In avian species, its application is constrained by flight-related skeletal adaptations and a relative scarcity of cancellous bone, which limit the availability of suitable graft material (Bennett and Kuzma, 1992; Darrow and Bennett, 2022). Reported autologous sources include cancellous bone from the proximal tibiotarsus in n large birds and terrestrial birds, corticocancellous bone harvested from the sternum/keel or ribs, and cortical bone obtained from unstable fracture fragments at the injury site (Bennett and Kuzma, 1992; Martin and Ritchie, 1994; Darrow and Bennett, 2022).

2. Objective

This study aimed to evaluate, through radiographic and histological analyses, the performance of F18 bioglass putty in comparison with an autologous cortical bone graft for repairing radial bone defects in chickens, used here as an avian experimental model. The hypothesis was that histological differences in tissue responses could occur between the two treatments. To the best of our knowledge, this biomaterial has not previously been tested in avian species.

3. Materials and Methods

Subjects and Experimental Environment

The methodology adopted in the present study was approved by the Ethics Committee on Animal Use of the School of Veterinary Medicine and Animal Science, Unesp, Botucatu campus (CEUA No. 0264/2022).

A total of 30 adult chickens (*Gallus gallus domesticus*) were used. The experiment was divided into distinct stages. In the first stage, the birds, weighing between 1.1 and 1.6 kg, were housed and separated in appropriate cages. They were provided with feed and water *ad libitum* for a 10-day adaptation period prior to the surgical procedure. After surgery, the birds were housed in an enclosed shelter measuring 3 × 3 meters during the nighttime and in an open area measuring 2 × 2 meters during the daytime.

Anesthetic and Surgical Procedures

Following the acclimation period, the chickens were subjected to a three-hour preoperative fast for both food and water. Body weight was then recorded, after which pre-anesthetic medication was administered, consisting of morphine (1 mg/kg) and midazolam (1 mg/kg), both given intramuscularly into the pectoral muscles. After a 10-minute interval, anesthesia was induced with isoflurane delivered via a face mask, followed by endotracheal intubation using a size 3 uncuffed tube. Anesthesia was maintained with isoflurane in oxygen.

Each chicken was positioned in dorsal recumbency with the wings extended to allow ventral access. Feathers on the right and left antebrachia were plucked, followed by antisepsis with 4% chlorhexidine and placement of surgical drapes. Through a ventral approach to the radius, the extensor carpi and pronator muscles were identified and carefully retracted to expose the underlying bone. A 0.5 cm segmental defect was then

created in the midshaft of both the right and left radii using an oscillating saw. The bone fragment obtained from the left radius during the creation of the segmental defect was kept in gauze moistened with blood until use. In the left radius, the segmental defect was filled with F18 bioglass putty (G1) (0.71 g). In the right radius (G2), the defect was filled with the cortical autologous bone fragment obtained from the left radius. The muscles and fascia were re-approximated using 4-0 polyglactin 910 suture in an interrupted cruciate pattern. The skin was closed with simple interrupted 4-0 monofilament nylon sutures.

During the postoperative period, analgesic and anti-inflammatory therapy was initiated with meloxicam (0.5 mg/kg), administered intramuscularly into the pectoral muscle once daily for three consecutive days. Antimicrobial therapy was instituted with enrofloxacin (30 mg/kg, orally), administered once daily for five days. Local wound management involved daily cleansing of the surgical site with 0.2% chlorhexidine solution, followed by the application of a protective bandage. Removal of the skin sutures occurred 7 days postoperatively.

Radiographic Examinations

Radiographic examinations of the antebrachia were performed under physical restraint. A mobile X-ray unit (EPX-F1600 B; Oxson®) in combination with an ExamVue DR® digital imaging system was used. Images were acquired using exposure settings of 3 mAs and 40 kV, with a focus-to-film distance of 80 cm. Assessments were conducted in the immediate postoperative period and at 15, 30, 50, 60, and 90 days postoperatively. For each evaluation, craniocranial and mediolateral projections of both the left and right forearms were obtained. The images were analyzed using RadiAnt DICOM Viewer software, version 2025.1 (64-bit), assessing the presence and displacement of the

material, the extent of bone defect filling, bone reactions, misalignment, and any increase in soft tissue volume.

Euthanasia and Histological technique

One chicken died spontaneously prior to completion of the experimental period and was excluded from the analysis. Chickens were euthanized at 50 days (n = 9), 90 days (n = 10), and 120 days (n = 10) following surgery. Initially, a combination of ketamine hydrochloride (30 mg/kg), xylazine hydrochloride (4 mg/kg), and tramadol (8 mg/kg) was administered intramuscularly. Once a deep anesthetic plane was achieved using an isoflurane mask, an intravenous bolus of potassium chloride was administered until cardiorespiratory arrest occurred.

For the histological study, the areas of bone defects—including the bone ends, the implanted biomaterial or bone graft, and the adjacent soft tissues—of the right and left radius were fixed in 10% buffered formaldehyde. The samples were decalcified using a 10% nitric acid solution. Subsequently, the bones were routinely processed in paraffin, sectioned into 5 μm-thick slices, and stained with hematoxylin and eosin. The processing of the samples was carried out at the Veterinary Pathology Laboratory of the Federal Institute of Education, Science, and Technology of Rondônia (IFRO), Colorado do Oeste campus. Samples obtained from the left and right radii were subjected to qualitative histological evaluation. The principal microscopic alterations were described and graded for intensity both qualitatively and quantitatively, as follows: absent (-; score 0), mild (+; score 1), moderate (++; score 2), and marked (+++; score 3). The parameters assessed comprised fibrocollagenous tissue proliferation, inflammatory infiltrate, and bone matrix formation. The foreign body reaction was recorded as present or absent.

Statistical Analysis

The variables fibrocollagen tissue proliferation, bone matrix formation, and inflammatory infiltrate —expressed as ordinal intensity scores (0 = no response, 1 = mild, 2 = moderate, 3 = intense)—were analyzed using a generalized linear mixed model (GLMM) with the PROC GLIMMIX procedure in SAS. For the ordinal variables, an ordered multinomial distribution with a cumulative logit link function was adopted, as it is appropriate for this type of data. The model included the fixed effects of treatment (*treat*), evaluation time points (*time*), and their interaction (*treat* × *time*), as well as the random effect of the chicken, to account for variability between experimental units. Differences between treatments were assessed through specific contrasts, and odds ratios were calculated by exponentiating the model coefficients. Additionally, predicted probabilities for each response category were obtained using the inverse link function (*ilink*). As the ordinal model produces cumulative probabilities, these were converted into marginal probabilities by computing the differences between consecutive cumulative levels. The resulting probabilities were then summarized by treatment or by treatment within each evaluation time point (when applicable), and the probability of higher-intensity responses (scores 2 and 3) was also calculated.

For the foreign body reaction variable—binary in nature (0 = absence, 1 = presence)—a generalized linear model was fitted assuming a binomial distribution and a logit link function. The effects of treatment, time, and their interaction were included in the model. The statistical significance of these effects was evaluated at the 5% probability level.

4. Results

Postoperative clinical evaluations

The anesthetic protocol employed enabled the surgical procedure to be carried out without complications and facilitated a prompt, satisfactory recovery. All birds resumed feeding approximately four hours after the intervention. Throughout the postoperative period, no alterations in locomotion or wing positioning were observed. Moreover, all chickens maintained normal food intake, and none exhibited self-trauma directed toward the operated area. The wounds progressed through the healing process without any adverse events.

Radiographic examinations

Immediately after surgery, radiographs revealed Bioglass F18 putty as a poorly demarcated radiopaque mass filling the bone defect. Its radiopacity progressively decreased over time, declining from full visibility at baseline to only 6.7% at 90 days. Bone proliferation originating from the fracture ends was absent or mild at all time points. Mild to moderate displacement of the bone ends was observed. In the immediate postoperative period, mild to moderate soft-tissue edema was identified. Although the degree of swelling decreased over time, residual edema was still evident during subsequent assessments.

Radiographic evaluation in the immediate postoperative period revealed the bone graft as a well-defined radiopaque structure with density comparable to the adjacent bone. The graft was detectable in all bone defects (100%) at each evaluation time point, with moderate to severe displacement observed in both the graft and the bone ends. Over time, a progressive reduction in radiographic density was noted, most prominently at the final evaluation. Concurrently, evidence of bone proliferation originating from the fracture ends was observed, indicating ongoing remodeling and integration of the graft material.

Soft-tissue swelling showed progressive reduction over time, with a predominance of absence at 90 days.

Figure 1 illustrates the findings for each group.

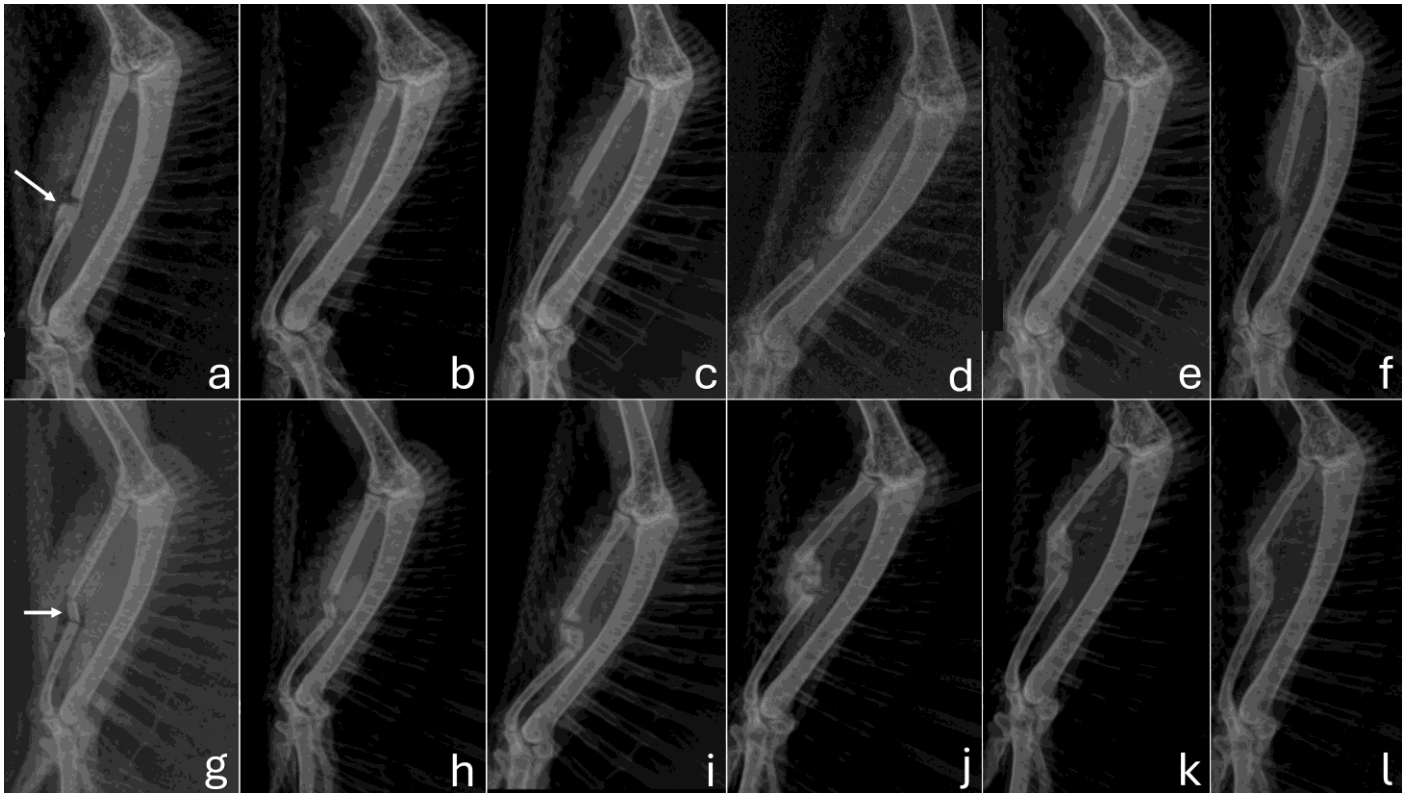

Figure 1. Mediolateral radiographic views of the antebrachium in chickens with radial bone defects, treated with F18 bioglass putty (G1 – left radius) or an autologous cortical bone graft (G2 – right radius). Immediate postoperative views (a, g) and at 15 (b, h), 30 (c, i), 50 (d, j), 60 (e, k), and 90 (f, l) days postoperatively. In G1, the F18 bioglass is visible in the immediate postoperative period as a radiopaque material (arrow). A decrease in radiopacity is observed over time, with absent or minimal bone proliferation from the fracture ends. In G2, the cortical bone graft appears as a well-defined radiopaque structure in the immediate postoperative period. A progressive reduction in radiopacity is observed, accompanied by bone proliferation from the fracture ends over time.

Histological analysis

In G1, multiple foci containing F18 bioglass fragments were observed, accompanied by fibrocellular proliferation, inflammatory infiltrates, and mild neovascularization predominantly localized within bone defect. The proliferative response consisted mainly of disorganized, low-density fibrocollagenous tissue interspersed by a moderate inflammatory infiltrate, composed primarily of histiocytes (Figure 2). Surrounding the bioglass particles, thin fibrous tissue (capsule) was observed, frequently surrounded by aggregates of lymphohistiocytic inflammation (Figure 3). Capsule morphology varied: in certain specimens, capsules were small and contained minimal bioglass material, whereas in others they encompassed nearly the entire defect. In the latter, the capsule interior appeared rarefied; in addition to reduced bioglass content, basophilic fragments consistent with necrotic debris were identified (Figure 4). Muscle fiber necrosis was common, particularly adjacent to fracture sites, and in some cases was associated with focal extensive necrosis and hemorrhage. Evidence of new bone matrix formation was minimal or absent in most of specimens.

In G2, similar to what was verified in G1, tissue proliferation, inflammatory infiltrate, and neovascularization were evident. The bone graft, which remained undegraded, was occasionally observed adhering linearly to the fracture ends or separated by fibrocollagenous tissue within the bone defect. These components were predominantly located adjacent to the bone ends, laterally, or between the fracture and the graft. The proliferative tissue consisted predominantly of fibrocollagenous tissue, frequently organized and dense. Interspersed within this fibrous tissue, a mild to moderate inflammatory infiltrate composed mainly of histiocytes was observed in most specimens. Bone matrix formation was noted between the graft and the fracture ends.

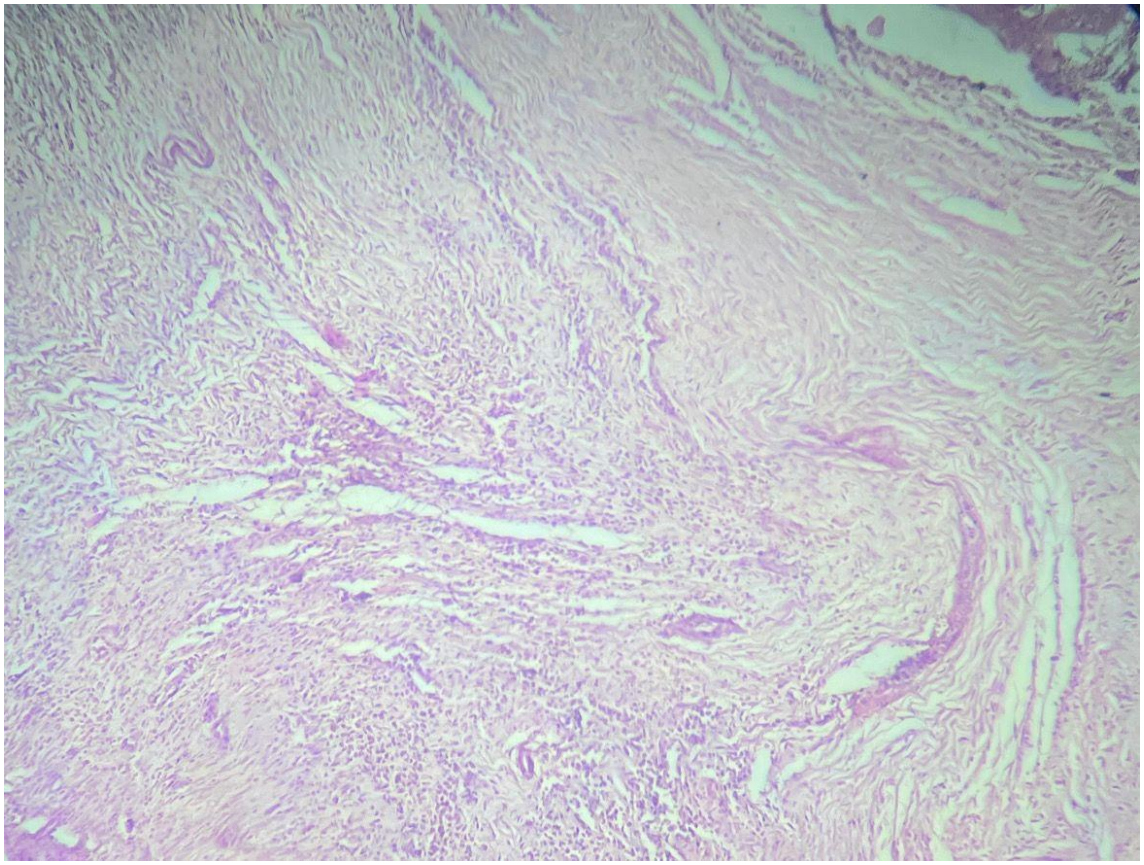

Figure 2. Representative histological section of a radial bone defect in a chicken treated with F18 bioglass putty, 50 days postoperatively. Area of intense fibrocollagenous proliferation associated with a marked inflammatory infiltrate composed of lymphohistiocytic cells, predominantly macrophages. Hematoxylin and eosin staining, 20×.

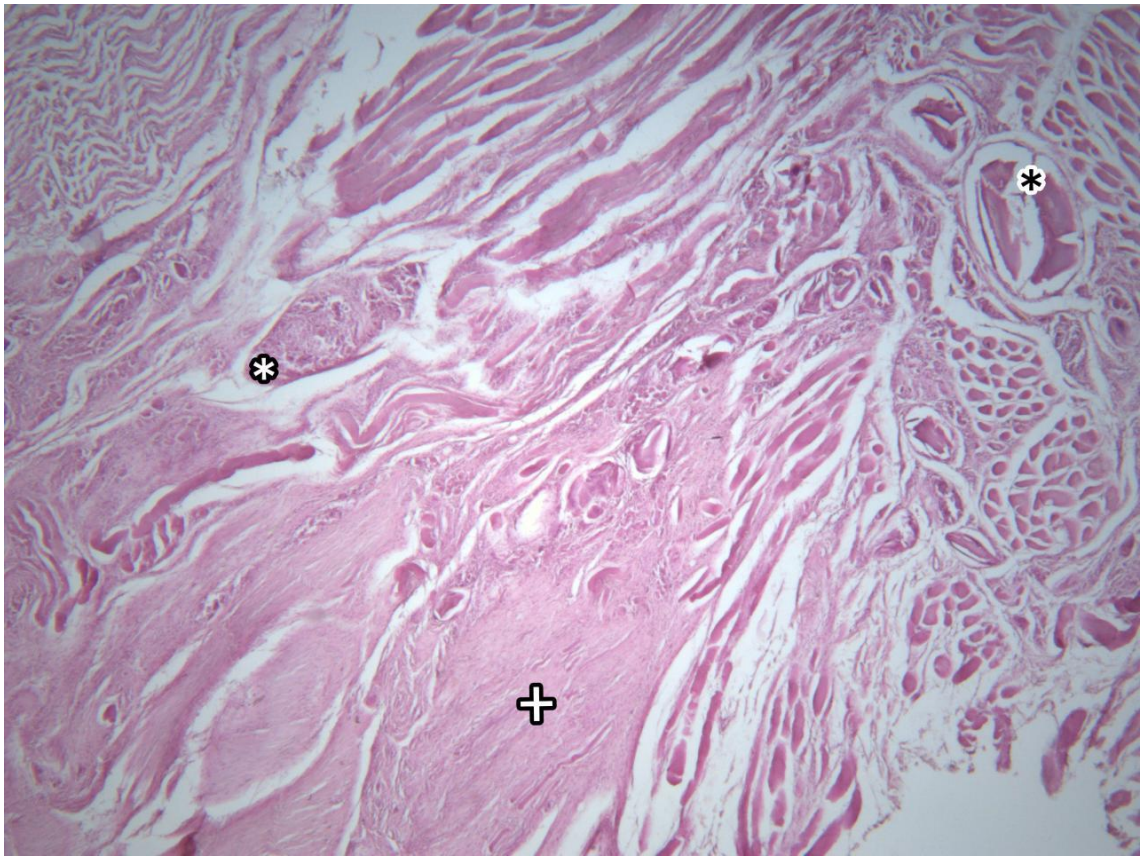

Figure 3. Representative histological section of a radial bone defect in a chicken treated with F18 bioglass putty, 90 days postoperatively. Area of fibrocollagenous proliferation (white cross) surrounding the bioglass putty. Residual bioglass particles are encased in a connective tissue capsule (black asterisk). Lymphohistiocytic inflammatory aggregates are present around small bioglass particles (white asterisk). Hematoxylin and eosin staining, 20×.

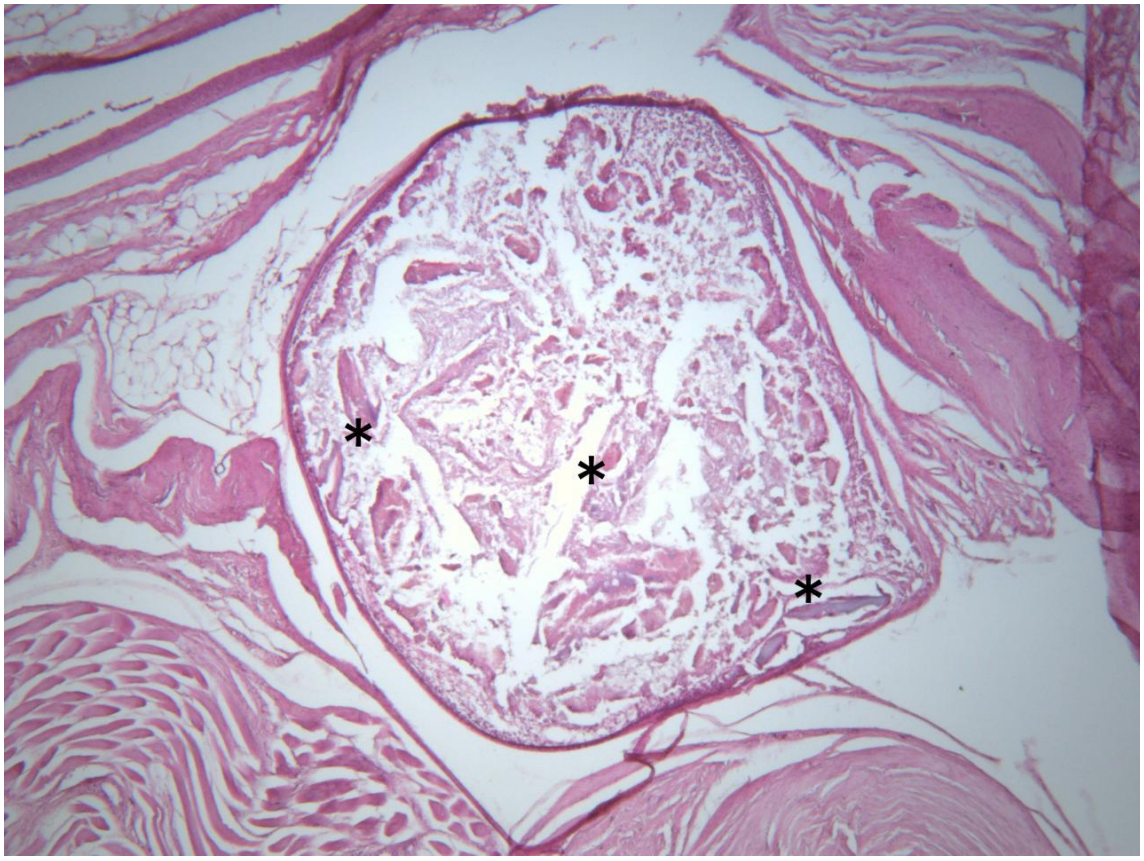

Figure 4. Representative histological section of a radial bone defect in a chicken treated with F18 bioglass putty, 120 days postoperatively. Bioglass fragments (asterisk) are surrounded by a thin fibrous tissue capsule, with necrotic tissue present inside the capsule. Hematoxylin and eosin staining, 20×.

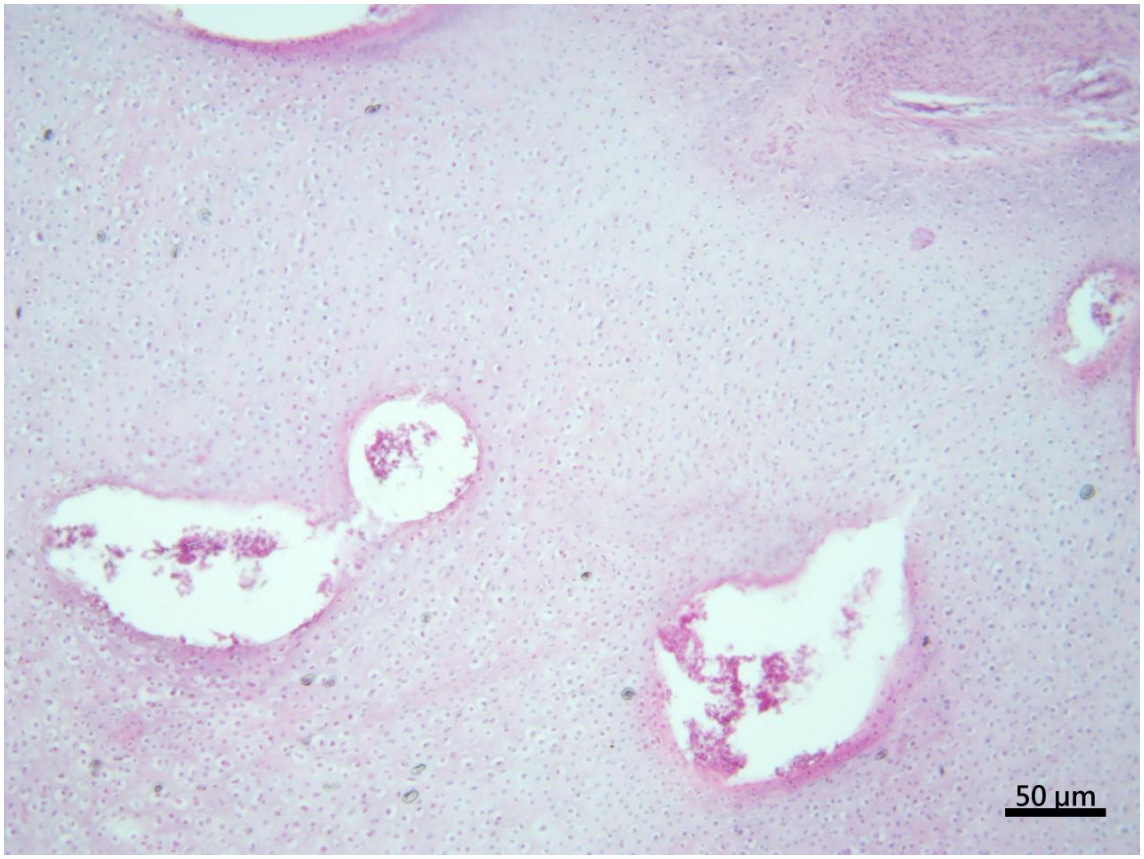

Figure 5. Representative histological section of a radial bone defect in a chicken treated with autologous bone graft, 90 days postoperatively. Note the intense formation of cartilaginous matrix adjacent to the graft area. Hematoxylin and eosin staining, 10×.

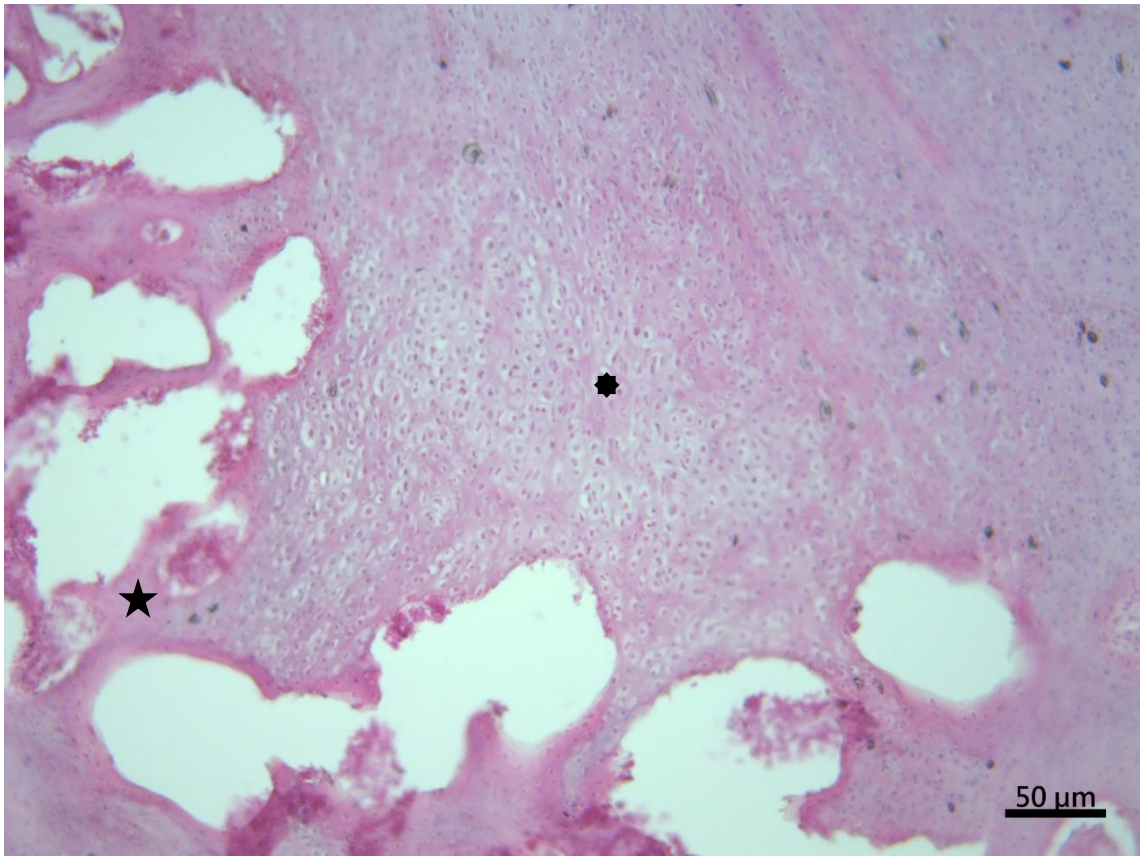

Figure 6. Representative histological section of a radial bone defect in a chicken treated with autologous bone graft, 90 days postoperatively. Intense formation of cartilaginous matrix (asterisk) is observed adjacent to the graft area, while bone metaplasia (star) is already evident in the peripheral region. Hematoxylin and eosin staining, 10×.

Statistics of histological analysis

Regarding fibrocollagen tissue proliferation**,** G1 increased the likelihood of more intense responses by approximately 6.4 times. Specifically, the probability of intense responses rose from 51% in G2 to 86% in G1. A significant treatment effect was observed ($p = 0.0037$), with G1 associated with greater response intensity compared to G2 (OR = 6.39). No significant effect of time point ($p = 0.0722$) or treatment × time interaction ($p = 0.3966$) was found, allowing treatment effects to be interpreted in an aggregated manner. Estimated probabilities indicated a higher frequency of high-intensity responses (scores 2 and 3) in G1 (86.0%) compared to G2 (51.4%). Moreover, G1 showed a greater likelihood of the highest intensity category (score 3), whereas G2 responses were predominantly concentrated in the moderate category.

In the evaluation of inflammatory infiltrate, both treatment and time point independently influenced the response. G1 showed an approximately 11-fold increase in the likelihood of more intense responses (scores 2 and 3), rising from 19% to 55%. In contrast, G2 exhibited a predominance of low responses (scores 0 and 1), accounting for 81% of cases. Response intensity was substantially higher at 50 days compared to 120 days. Specifically, the likelihood of an intense response at 50 days was 22.9 times greater than at 120 days, and 14.1 times greater than at 90 days. No significant difference was observed between responses at 90 and 120 days. The maximum effect occurred at 50 days, followed by a marked decline, regardless of treatment. Significant effects of treatment ($p = 0.0005$) and time point ($p = 0.0010$) were verified, with no interaction between these factors ($p = 0.7648$). G1 had a higher response intensity than G2 (OR = 11.35), with estimated probabilities indicating a greater frequency of high-intensity responses (scores 2 and 3) in G1 (55.5%) compared to G2 (18.8%). In terms of time-

dependent changes, high-intensity responses were approximately 14 times more likely at 50 days than at 90 days ($p = 0.0014$), and 23 times more likely than at 120 days ($p = 0.0004$), while no difference was detected between 90 and 120 days ($p = 0.4491$). The estimated probabilities showed a marked difference between the groups. G2 demonstrated a higher frequency of low-intensity responses (scores 0 and 1; 81.2%), whereas G1 exhibited a higher occurrence of high-intensity responses (scores 2 and 3; 55.5%). Over time, the highest response intensity was observed at 50 days, with a probability of intense responses of 69.5%, followed by a decline at 90 days (26.2%) and 120 days (17.8%). At 120 days, low-intensity responses predominated.

For bone matrix formation, the probability of greater intensity in G1 is approximately 95.5% lower than in G2 ($1 - 0.0447$), indicating that G2 is 22.4 times more likely to present high scores than G1. G2 shows a predominance of more intense responses, whereas G1 is characterized by predominantly less intense responses. Due to the low frequency of the highest intensity category (score 3), the scores were grouped into three levels (0, 1, and ≥ 2) to ensure model convergence and stability of the estimates. There was a significant treatment effect ($p = 0.0003$), with G1 showing a lower likelihood of higher scores compared to G2 (OR = 0.045). The predicted probabilities indicated a higher frequency of intense responses in G2 (50.1%), whereas G1 showed a predominance of low-intensity responses, with only a 12.0% probability of high scores.

No significant effects of treatment ($p = 0.9660$), time point ($p = 0.8918$), or their interaction ($p = 0.8022$) were observed for the foreign body reaction, indicating no difference in the occurrence of the evaluated response between the groups.

The statistical data are summarized in Tables 1 and 2 and illustrated in Figures 1 and 2.

Table 1. Probability of high-intensity responses (high scores), odds ratios (OR), and statistical significance for radial bone defects treated with F18 bioglass putty (G1) and cortical autograft (G2).

Variables	G1 (%)	G2 (%)	OR (G1 vs G2)	P-value	Significance
Fibrocollagenous tissue proliferation	86.0	51.4	6.39	0.0037	**
Inflammatory infiltrate	55.5	18.8	11.35	0.0005	***
Bone matrix formation	12.0	50.1	0.045	0.0003	***
Foreign body reaction	—	—	—	0.9660	not significant

$p < 0.05$; ** $p < 0.01$; *** $p < 0.001$

Table 2. Probability of high-intensity responses of the inflammatory infiltrate (high scores) over time points and multiple comparisons.

Time points (days)	Probability (%)	Comparison	Odds ratios (OR)	P-value	Significance
50	69.5	—	—	—	—
90	26.2	50 vs 90	14.1	0.0014	**
120	17.8	50 vs 120	22.9	0.0004	***
—	—	90 vs 120	0.62	0.4491	not significant

$p < 0,05$; ** $p < 0,01$; *** $p < 0,001$

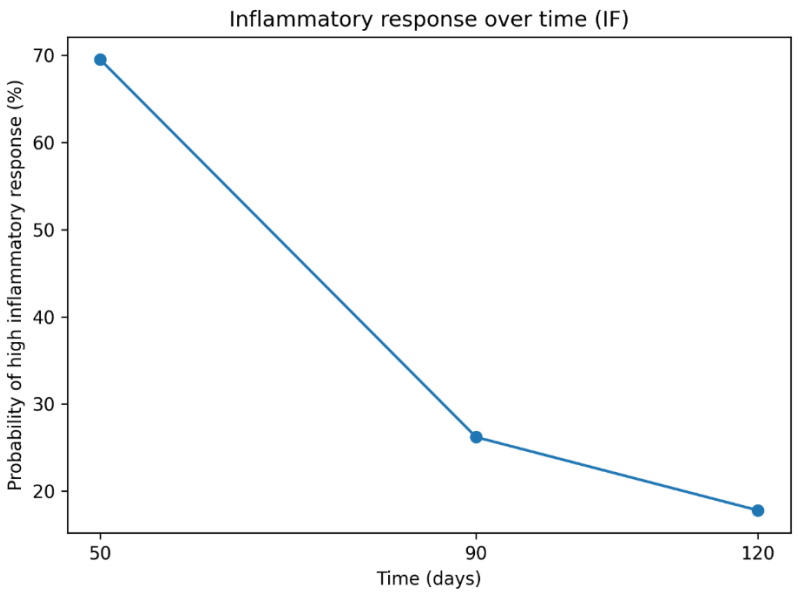

Figure 1. Probability (%) of high-intensity inflammatory infiltrate (high scores) over time points. A marked reduction is observed between 50 and 90 days, followed by stabilization from 90 to 120 days.

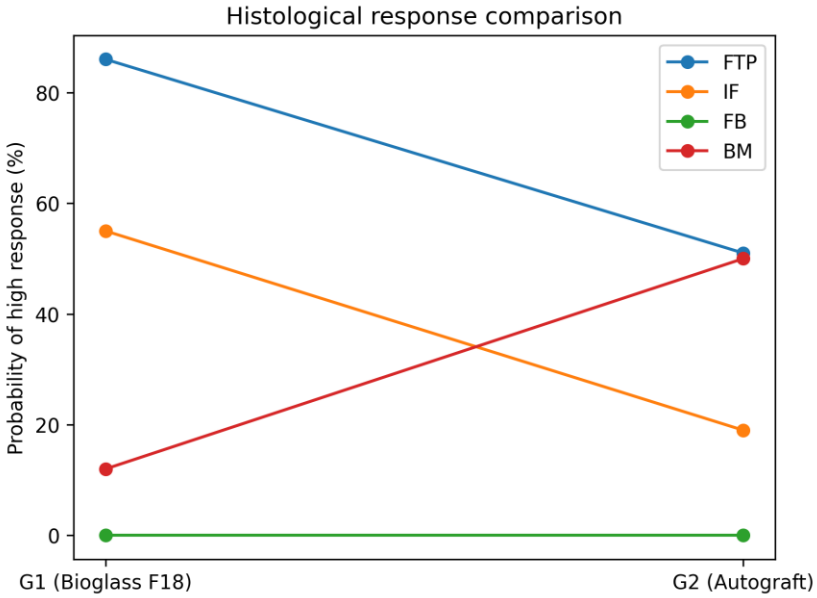

Figure 2. Histological response comparison between G1 (bioglass F18) and G2 (autologous cortical bone graft). G1 showed higher probabilities of high-intensity responses for FTP (fibrocollagen tissue proliferation) and IF (inflammatory infiltrate), whereas G2 presented higher probability of BM (bone matrix formation). No differences were observed for FB (foreign body reaction).

5. Discussion

Histological analysis supported the hypothesis, revealing distinct differences in tissue responses between G1 and G2 throughout the entire observation period. The limited availability of suitable autologous bone in avian species, combined with the morbidity associated with donor site harvesting (Bennett and Kuzma, 1992; Martin and Ritchie, 1994; Darrow and Bennett, 2022), underscores the need to explore biomaterials, as undertaken in this study.

Radiographically, G1 showed minimal or no bone growth from the fracture ends, with bioglass F18 putty exhibiting poor definition and low radiopacity, which progressively decreased over time. These findings were consistent with those described in rabbit bone defect models, where no signs of bone formation from the fracture ends were detected and radiographic changes were associated with the biodegradation of the bioglass F18 putty (Silva Júnior et al., 2024). In contrast, the cortical bone autograft (G2) was still visible at the final evaluation, 90 days postoperatively. Due to the dense structure of cortical grafts, revascularization and remodeling are limited, with incorporation occurring through new bone deposition over a necrotic core following osteoclast-mediated resorption, a process that may extend over several years depending on graft dimensions and implantation site (Wang and Yeung, 2017). The gradual increase in radiographic lucency of the graft over time, as observed in the present study, may suggest the initiation of resorption or incorporation (Ocksrider et al., 2020). Furthermore, bone proliferation at the fracture ends was evident, demonstrating ongoing remodeling and integration of the graft material, even in cases where graft displacement had occurred. The adjacent intact ulna did not provide sufficient stability for the radius and bone graft. Therefore, internal fixation should be considered in future investigations.

G1 exhibited a significantly higher incidence of intense fibrocollagen proliferation compared to G2, with more frequent maximum-intensity responses. The early phase of fracture healing is characterized by angiogenesis, osteoid deposition, and fibrocollagen formation, whereas the subsequent phase involves differentiation of mesenchymal cells into chondrocytes, which synthesize cartilage matrix components such as type II collagen and proteoglycans (Chen and Alman, 2009). The continued presence of fibrocollagen proliferation in G1 indicates that, within the context of the present study, the F18 bioglass putty may have had limited effectiveness in promoting a transition toward chondrogenesis. These findings differ from those of a previous study on bone defects in rabbits, where dense fibrocollagenous tissue was accompanied by the presence of chondroid and osteoid matrices (Silva Júnior et al., 2024).

In the present study, the intensity of the inflammatory response was influenced by both treatment type and time. The strongest responses were observed at 50 days**,** followed by a sharp decline at 90 and 120 days. During the early stages of bone healing, a cortical autograft is gradually replaced—primarily through osteoclastic activity—after hematoma formation and the initiation of the inflammatory reaction (Wang and Yeung, 2017). This explains the inflammatory response detected in group G2. In contrast, the higher inflammatory infiltrate observed in G1 may be related to the use of F18 bioglass in putty format. In a rabbit radius segmental defect model designed to induce membrane formation, F18 bioglass putty triggered a pronounced mixed inflammatory infiltrate at 21 days post-surgery, which diminished to mild levels by 42 days (Silva Júnior et al., 2024). Conversely, another study assessing fibrous glassy scaffolds composed of the SiO_2–Na_2O–K_2O–MgO–CaO–P_2O_5 system, implanted into tibial defects in Wistar rats, reported only mild inflammation at 15 days, and an absence of inflammatory reaction at 30 and 60 days postoperatively.

G2 exhibited significantly higher bone matrix formation intensity than G1, being about 22 times more likely to present strong responses. The findings align with the established evidence that autologous bone grafting remains the gold standard for repairing bone defects, due to its synergistic osteoconductive, osteoinductive, and osteogenic properties (Wang and Yeung, 2017). In the present study, the bone graft source — a bone fragment obtained from the contralateral radius during bone defect induction — differed from clinical scenarios in which cortical bone is obtained opportunistically from fragments at the injury site during fracture management (Bennett and Kuzma, 1992; Martin and Ritchie, 1994; Darrow and Bennett, 2022). This controlled harvesting method ensured consistent graft quality, minimized variability in structural integrity, and eliminated the influence of trauma-related factors.

G1 showed predominantly low-intensity scores for bone matrix formation, with only a 12% probability of high scores compared to 50% in G2. The bioactivity of glass scaffolds is strongly influenced by chemical composition, as well as the microstructural characteristics of their pore architecture and fabrication method (Fu et al., 2011; El-Rashidy et al., 2017). A study of F18 bioglass putty applied to rabbit bone defects detected areas of chondroid matrix and osteoid matrix (Silva Júnior et al., 2024). On the other hand, a fibrous glassy scaffold based on the SiO_2–Na_2O–K_2O–MgO–CaO–P_2O_5 compositional system demonstrated pronounced bioactivity and reactivity in *in vitro* evaluation, and in tibial defects of Wistar rats, the regenerated bone was comparable to that observed in the control group (Gabbai-Armelin et al., 2017).

A foreign body reaction was detected in both groups. In general, implantation of a biomaterial triggers an inflammatory response as the body's reaction to foreign material, which may be either detrimental or benign (Dickenson et al., 2026). Given the minimal immunogenicity of cortical autograft and the comparable foreign body reactions observed

in both groups, the results indicate that F18 bioglass possesses a similarly favorable biocompatibility profile.

The unique structural and physiological characteristics of avian bones (González, 2019) may have influenced the degradation dynamics, ion release, and integration of F18 bioglass in ways that differ from those in mammalian models. In addition, one limitation of this study was that only radiographic assessment was employed. The incorporation of advanced quantitative imaging modalities and molecular analytical techniques could have provided more accurate and comprehensive evaluations of the healing process.

Conclusion

In this avian radial defect model, autologous cortical bone graft and F18 bioglass putty exhibited distinct repair patterns, with the graft favoring bone matrix formation and the bioglass associated with greater fibrocollagen proliferation and inflammatory responses.

References

Bennett RA, Kuzma AB. Fracture management in birds. *J Zoo Wildl Med*. 1992;23(1):5-38.

Chen Y, Alman BA. Wnt pathway, an essential role in bone regeneration. *J Cell Biochem*. 2009;106(3):353-62. doi:

Darrow B, Bennett RA. Avian orthopedics. In: Bennett RA, Pye GW (Editors). *Surgery of exotic animals.* Hoboken: John Wiley and Sons, 2022. p.112-153.

Dickenson ME, Oakes RS, Morris AH. Don't judge an implant by its cover: how the foreign body response and fibrotic capsule might be harnessed for good. *NPJ Biomed Innov*. 2026;3(1):3.

El-Rashidy AA, Roether JA, Harhaus L, Kneser U, Boccaccini AR. Regenerating bone with bioactive glass scaffolds: A review of in vivo studies in bone defect models. *Acta Biomater*. 2017;62:1-28.

Ellakwa DEl-S, Abu-Khadra AS, Ellakwa TE. Insight into bioactive glass and bio-ceramics uses: unveiling recent advances for biomedical application. *Discov Mater*. 2025;5:78.

Fu Q, Saiz E, Rahaman MN, Tomsia AP. Bioactive glass scaffolds for bone tissue engineering: state of the art and future perspectives. Mater Sci Eng C Mater Biol Appl. 2011;31(7):1245-1256.

Gabbai-Armelin PR, Souza MT, Kido HW, et al. Effect of a new bioactive fibrous glassy scaffold on bone repair. *J Mater Sci Mater Med*. 2015;26(5):177.

Gabbai-Armelin PR, Souza MT, Kido HW, et al. Characterization and biocompatibility of a fibrous glassy scaffold. *J Tissue Eng Regen Med*. 2017;11(4):1141-1151.

González MS. Skeletal Bone Structure and Repair in Small Mammals, Birds, and Reptiles. *Vet Clin North Am Exot Anim Pract.* 2019;22(2):135-147.

Marin CP, Crovace MC, Zanotto ED. Competent F18 bioglass-Biosilicate® bone graft scaffold substitutes. *J Eur Ceram Soc*. 2021;41(15):7910-7920.

Martin H, Ritchie BW. Orthopedic surgical techniques. In: Ritchie BW, Harrison GJ, Harrison LR (Editors). *Avian medicine: principles and application*. Lake Worth: Wingers Publishing, 1994. p. 1138-1169.

Nozari LB, Oliveira HFFE, Marinho GD, Santiago Junior JF, Marques MM, Deboni MCZ, Ferraz EP. Bioactive glasses as bone substitutes for animal critical defects: A systematic review. *Braz Dent J.* 2025;36:e236464.

Ocksrider J, Boden AL, Greif DN, Hernández R, Jose J, Pretell-Mazzini J, Subhawong T, Foremny GB, Singer A, Quinnan SM. Radiographic evaluation of reconstructive surgery for segmental bone defects: What the radiologist should know about distraction osteogenesis and bone grafting. *Clin Imaging.* 2020;67:15-29.

Silva Júnior JIS, Rahal SC, Coris JGF, Silva BMD, Brasileiro FCDS, Nascimento D, Lacerda ZA, Silva JPD, Mamprim MJ, Souza MT. Use of F18 bioglass putty for induced membrane technique in segmental bone defect of the radius in rabbits. *Acta Cir Bras*. 2024 May 24;39:e392424.

Souza \MT, Zanotto ED, Peitl-Filho O. 2013; Vitreous composition, bioactive glassy fibers and tissues. *Patent Application No. BR 10 2013 020961 9*; Universidade Federal de São Carlos, Brazil, Patent Application No. BR 10 2013 020961 9.

Souza MT, Rennó ACM, Peitl O, Zanotto ED. New highly bioactive crystallization-resistant glass for tissue engineering applications. *Transl Mater Res.* 2017;4:014002.

Wang W, Yeung KWK. Bone grafts and biomaterials substitutes for bone defect repair: A review. *Bioact Mater.* 2017;2(4):224-247.

6. Orientações e disciplinas ministradas com a respectiva carga horária e/ou a realização de atividades de extensão

Informamos que o aluno desenvolveu seu pós-doutoramento sem apoio financeiro, devido à não concessão de bolsa para o projeto. No entanto, durante o período em que havia previsão de vigência de bolsa, o pesquisador participou de concurso público no Instituto Federal de Educação, Ciência e Tecnologia de Rondônia – Campus Jaru (IFRO), sendo aprovado para o cargo de docente da instituição.

Em razão dessa aprovação e da consequente mudança de local de atuação, não foi possível ministrar disciplinas ou realizar atividades de extensão vinculadas à Faculdade de Medicina Veterinária e Zootecnia da Universidade Estadual Paulista (FMVZ – Unesp, Botucatu). Ressalta-se, contudo, que a experiência e a qualificação adquiridas ao longo do pós-doutoramento constituíram um diferencial significativo para a aprovação no referido concurso público.

A presença de um docente egresso da FMVZ/Unesp na condução da nucleação no IFRO assegura a integração de competências acadêmicas e científicas, promovendo sinergias entre instituições e beneficiando a formação de novos pesquisadores.